Measurements of turbine blade temperature in an operating aero engine using thermographic phosphors

Thomas P Jenkins[1,4], **Cecil F Hess**[1], **Stephen W Allison**[2] **and Jeffrey I Eldridge**[3]

[1] MetroLaser, Inc., Laguna Hills, CA, United States of America
[2] Emerging Measurements Company, Collierville, TN, United States of America
[3] NASA Glenn Research Center, Cleveland, OH, United States of America

E-mail: tjenkins@metrolaserinc.com

CrossMark

Abstract
A diagnostic method is introduced for non-contact temperature measurements on the surface of a rotating turbine blade in an operating engine using laser-induced excitation of thermographic phosphor coatings on the blades. Temperature measurements of between 513 °C and 767 °C are demonstrated on a pair of moving turbine blades with a fiber optic probe mounted in the engine at rotational speeds of between 28 000 and 32 750 RPM. The method involves measuring the decay times of laser-induced luminescence from two thermographic phosphors applied to thermal barrier coatings on the turbine blades, one with a short, temperature-sensitive, decay time and the other with a longer, less temperature-sensitive decay time. The phosphors are excited by laser pulses at a wavelength of 355 nm and luminescence is collected at 456 nm from one phosphor and at 485 nm from the other. The effects of motion on the temperature determination are removed by using a ratio of luminescence intensities of the two phosphors. Potential interferences from chemiluminescence, particles, hot surfaces, and reflections within the engine are avoided by limiting the detection to a narrow spectral window around the luminescence wavelengths. The data exhibit high signal-to-noise ratios and the measured temperatures are within the expected range for this engine.

Keywords: thermographic phosphors, gas turbine diagnostics, turbine blade thermometry, laser-induced luminescence

(Some figures may appear in colour only in the online journal)

1. Introduction

Jet engines of the future will need to have increased efficiencies to meet the challenges of rising fuel costs and increasing emissions regulations. Engine performance is strongly dependent on the temperatures attained at the turbine inlet, which are typically limited by material degradation of the turbine blades. It is desirable to operate at the highest allowable temperatures that the turbine blades can withstand to maximize efficiency [1]. Under such conditions, methods for monitoring turbine blade temperature are needed to ensure that the material limits are not exceeded. Current methods for measuring blade temperature are mainly based on optical pyrometery, which can suffer from errors inherent to the gas turbine operating environment [2]. These errors can be substantial and are due to signal contamination from reflections, uncertainty in emissivity, and the fouling of windows by soot and other particulates.

Thermographic phosphors applied to the thermal barrier coatings (TBCs) of turbine blades have shown promise as an alternative method of temperature measurement that may not be as prone to error [3–10]. In luminescence lifetime methods, a phosphor is excited by a light source and the time for the resulting luminescence to decay is an indicator of the

temperature. The method can be made robust against a bright flame background by selecting a phosphor with luminescence wavelengths that are shorter than the prominent thermal emission wavelengths so that the infrared background can be spectrally filtered out.

Thermographic phosphor temperature sensors have been applied to TBCs in turbine engines since the early nineties [11]. The method can involve either applying the phosphor to the surface of the TBC [3, 6] or embedding it as a thin layer within the coating [4, 5, 12–14]. The excitation light source is typically a laser or light emitting diode. In addition to the luminescence lifetime approach, a change in spectral distribution of the luminescence with temperature may also be employed as the sensing mechanism. However, the luminescence lifetime approach is generally found to be more accurate, especially at high temperatures, since lifetime based techniques can provide a higher level of immunity to window fouling and changes in emissivity and tend to have greater sensitivity compared to spectral intensity techniques [3]. Temperature measurements have been demonstrated using luminescence lifetime-based phosphor thermometry on a TBC-coated superalloy substrate at temperatures of up to 1400 °C in hot gas flows from a jet fuel spray flame [15], and on a nozzle guide vane at up to 1250 °C in a turbojet engine exhaust [16, 17]. Allison *et al* [8] demonstrated temperature measurements using a thulium-based phosphor on a stator vane in an operating engine using a fiber optic probe and found good temperature sensitivity during start-up and shut-down phases of engine operation. A later effort to measure temperatures on a nozzle guide vane on a full-scale aero gas turbine revealed challenges caused by high background emission levels for blades near the combustor [18]. Feist *et al* [19] demonstrated phosphor thermometry measurements of temperatures near 500 °C on a moving turbine blade at 13 000 RPM in an operating aero engine using free-space optics to couple the laser into the engine and convey the luminescence signal out. The optics in their experiment were external to the engine, relying on alignment of components placed 0.4 m from the measurement location.

In the present work, we report on a demonstration of turbine blade temperature measurements in a full-scale aircraft turbofan engine using a fiber optic probe attached to the engine that does not rely on the alignment of beams from external sources into the engine. The effects of motion are compensated for by taking the ratio of signals from two phosphors, one with a luminescence lifetime that is short relative to the blade passing duration and the other with a longer relative lifetime. Interference from naturally present luminosity of the gases and hot surfaces in the engine is avoided by selecting phosphors with short wavelength emission bands.

2. Methods

2.1. Fundamental concepts

The method involves measuring the luminescence decay lifetime of a phosphor after a short laser excitation pulse. Higher temperatures result in shorter decays since a greater number of
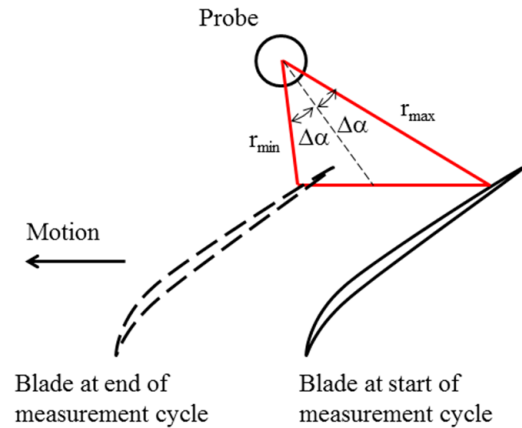

Figure 1. Location of the probe relative to a moving blade in an engine.

energy transition pathways are active. Since the luminescence is confined to specific spectral bands, it is possible to avoid interference from background laser light, blackbody radiation, and reflections of the flame. Furthermore, the technique is based on a relative comparison of signal levels at various delays, so absolute intensity variations, such as those due to the accumulation of soot or other deposits on windows, do not hinder the measurement significantly. An advantage of the phosphor thermometry technique over conventional pyrometry is that the emissivity of the coating material, which may vary during engine operation due to oxidation or accumulation of soot, does not need to be known.

A challenge when making time-varying optical measurements in an operating engine is that the collection efficiency changes as the blade moves. Figure 1 shows the position of the probe relative to the blade representing the experimental configuration used, in which the suction side of the blade was interrogated. The blade positions at the start and end of the measurement cycle are shown. At the start of the cycle, the blade enters the field of view and the solid angle of collection is given by $\Omega = A/r_{\max}^2$, where A is the area of the laser spot on the blade and $r_{\max}$ is the probe-to-spot distance. As the blade moves through the field of view, the distance decreases, becoming $r_{\min}$ where it exits the field of view. Thus, the collection efficiency, which is proportional to Ω, increases by a factor of $(r_{\max}/r_{\min})^2$ throughout the measurement cycle. For the present probe, the angle $\Delta\alpha$, shown in figure 1, was 20°, and the nominal distance from the probe to the spot was 25 mm. This results in a ratio $r_{\max}/r_{\min}$ of 1.5, or a ratio $\Omega_{max}/\Omega_{min}$ of 2.3. Therefore, the signal level can be expected to increase by a factor of 2.3 during the measurement period.

To account for this variation in collection efficiency with blade position, two phosphors were used, one with a luminescence decay lifetime that was short compared to the measurement window, and the other with a decay lifetime that was long. Measurements of luminescence were obtained from two different turbine blades adjacent to each other, each coated with a different phosphor. By obtaining measurements from both phosphors at a given engine condition, the temperature was related to the ratio of intensities, which is independent of the blade motion.

The signal from phosphor i, denoted S_i, is modeled as a function of time, t, as

$$S_i = \eta_{q,i}\eta_{\text{tr},i} n\sigma_i(T)\,\Omega(t)\,E_{\text{L}}\exp\left(-\frac{t}{\tau_i(T)}\right), \qquad (1)$$

where $\eta_{q,i}$ is the quantum efficiency of the detector, $\eta_{\text{tr},i}$ is the transmission efficiency of the optical system, $\sigma_i(T)$ is the temperature dependent luminescence cross section per active ion (accounting for absorption and emission), n is the number of active ions, $\Omega(t)$ is the time dependent solid angle of collection, E_{L} is the laser pulse energy, and $\tau_i(T)$ is the temperature dependent luminescence lifetime. Note that in equation (1), the only quantities that depend on temperature are σ_i and τ_i.

Letting S_1 and S_2 be the short- and long-lifetime phosphors, respectively, their ratio, R, is

$$R = \frac{S_1}{S_2} = \frac{\eta_{q,1}\eta_{\text{tr},1}n_1\sigma_1}{\eta_{q,2}\eta_{\text{tr},2}n_2\sigma_2}\exp\left(-\left(\frac{1}{\tau_1}-\frac{1}{\tau_2}\right)t\right). \qquad (2)$$

Note that the dependence on solid angle, and therefore the effects of blade motion, have canceled out in the ratio of signals. Equation (2) shows that if each phosphor exhibits single exponential decay behavior, then the ratio of the signals, R, also exhibits single exponential decay behavior. The effective decay time for R can be defined as $\tau_{\text{R}} = (1/\tau_1 - 1/\tau_2)^{-1}$. Note that τ_{R} is the decay time for the signal ratio, which is not equal to the ratio of the phosphor decay times. Because R has no dependence on blade motion, τ_{R} can be simply obtained by fitting a single exponential to the decay of R. Basing the temperature measurement on the decay of R provides the significant simplification of eliminating the requirement of determining the effect of blade motion on the individual phosphor decays. Thus, there is no need to determine the YAP:Tm decay time by removing the effect of motion. Rather, the goal is to determine τ_{R}, which is not actually a lifetime but a mathematical construct from the two decay times. As shown by equation (2), the effects of motion are fully removed by taking the signal ratio.

The absolute temperature sensitivity, S_{abs}, and relative temperature sensitivity, S_{rel}, of τ_{R} are given by:

$$S_{abs} = \frac{d\tau_{\text{R}}}{dT} = \frac{\frac{1}{\tau_1^2}\frac{d\tau_1}{dT} - \frac{1}{\tau_2^2}\frac{d\tau_2}{dT}}{\left(\frac{1}{\tau_1}-\frac{1}{\tau_2}\right)^2} \qquad (3a)$$

$$S_{rel} = \frac{1}{\tau_{\text{R}}}\frac{d\tau_{\text{R}}}{dT} = \frac{\frac{1}{\tau_1^2}\frac{d\tau_1}{dT} - \frac{1}{\tau_2^2}\frac{d\tau_2}{dT}}{\frac{1}{\tau_1}-\frac{1}{\tau_2}}. \qquad (3b)$$

Temperature sensitivity by itself is not a good predictor of temperature measurement precision because the signal-to-noise ratio (ratio of signal mean to standard deviation) also has a large effect on measurement precision. An estimate of temperature measurement precision can then be given by the noise equivalent temperature difference (NETD) [15, 20], given by:

$$\text{NETD} = \frac{\sigma_{\tau_{\text{R}}}}{S_{abs}} = \frac{\sqrt{\frac{\sigma_{\tau_1}^2}{\tau_1^4} + \frac{\sigma_{\tau_2}^2}{\tau_2^4}}}{\frac{1}{\tau_1^2}\frac{d\tau_1}{dT} - \frac{1}{\tau_2^2}\frac{d\tau_2}{dT}}, \qquad (4)$$

where $\sigma_{\tau_{\text{R}}}$, $\sigma_{\tau 1}$, and $\sigma_{\tau 2}$ are the standard deviations of τ_{R}, τ_1, and τ_2, respectively. NETD is essentially the temperature range associated with the uncertainties in τ_1 and τ_2. This expression can be used to minimize temperature measurement uncertainty by selecting phosphors that will minimize the numerator and maximize the denominator. To maximize the denominator of equation (4), the first term of the denominator should be as large as possible while the second term should be as small as possible. Therefore, it is desirable to maximize the temperature sensitivity of phosphor 1 (in the temperature range of interest) while minimizing the temperature sensitivity of phosphor 2. The terms in the denominator also reveal that increasing τ_2 has the beneficial effect of decreasing NETD, while increasing τ_1 has the undesirable effect of increasing NETD. Therefore, it is beneficial to select a long luminescence lifetime for phosphor 2 and a short lifetime for phosphor 1. Tm-doped yttrium aluminum perovskite (YAP:Tm) was chosen as phosphor 1 because it has a short luminescence lifetime, reasonable temperature sensitivity, and a wide temperature range. The wide temperature range necessarily means that the temperature dependence cannot be too steep, but the sensitivity is reasonable and this phosphor was selected as a compromise. Dy-doped yttrium aluminum garnet (YAG:Dy) was chosen as phosphor 2 because it has a long luminescence lifetime and minimal temperature sensitivity within the range of interest. These considerations, along with the requirement of short emission wavelengths, were the rationale for selecting the two phosphors used.

2.2. Calibration

Calibration consisted of measuring luminescence decay times of the two phosphors over the range of relevant temperatures. Although no blade motion was involved in the furnace calibration measurements, τ_{R} could still be accurately determined from the decay times τ_1 and τ_2 obtained from the individual phosphor decay curves by the relationship as $\tau_{\text{R}} = (1/\tau_1 - 1/\tau_2)^{-1}$. The blade to be calibrated was placed inside a box furnace (MTI model KSL1100X) on an alumina stand. Holes in the door of the furnace allowed optical access to the blade. The beam was generated by a pulsed laser with a wavelength of 355 nm and pulse duration of 10 ns and had a diameter of about 1 mm, striking the sample at a 45° angle from the surface normal. The laser pulse had a duration of about 10 ns, a repetition rate of 200 Hz, and an energy of about 50 μJ. Luminescence from the measurement spot was collected with a 50 mm-diameter lens of focal length 100 mm onto the face of a fiber optic with a core diameter of 600 μm, which conveyed it to a photomultiplier tube (Hamamatsu R3896) for measurement.

The 200 Hz laser pulse repetition rate used for the calibration was substantially greater than the 10 Hz rate that was used for the engine measurements, to be described later. The higher pulse rate was selected because this facilitated a more precise calibration, since it enabled collecting a larger number of decay curves over which to average. Although the pulse energy was lower (50 μJ for the calibration versus 3 mJ for the
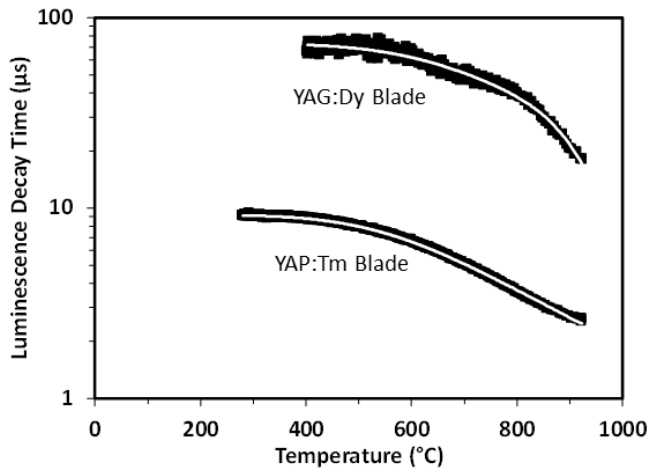
Figure 2. Luminescence lifetime versus temperature for two phosphor-coated turbine blades, showing two subranges for each that exhibited exponential decay.

engine measurement), this was offset by a smaller spot size (1 mm for the calibration versus 7 mm for the engine measurement), resulting in the laser fluence being the same to within a factor of two. Measurements to investigate the effect of laser fluence on luminescence lifetime were performed at fluences ranging from 5 to 10 mJ cm^{-2}, encompassing the calibration and engine measurement conditions. These measurements revealed that the measured lifetime changed by less than 2% over this range for both phosphors.

The collected light conveyed by the fiber to the photomultiplier tube passed through a bandpass filter centered at 456 nm for the YAP:Tm phosphor and 485 nm for the YAG:Dy phosphor. The same photomultiplier tube was used for both measurements, and one measurement was performed at a time. The same gain settings were used on the photomultiplier tube for calibration and engine measurements and the signal levels were similar. Signals from the photomultiplier tube were digitized at a rate of 100 MSamples s^{-1} with an oscilloscope (Tektronix TDS3032) and transferred to a computer via a GPIB interface. Records of 10 000 data points were acquired for each laser pulse, for a total record duration of 100 μs.

The calibration procedure consisted of heating the furnace to a temperature of 920 °C, then turning off the furnace and acquiring luminescence decay records as it cooled naturally. In post processing, a single exponential function of time of the form $S = S_0 e^{-t/\tau}$ was fit to the data over the range 1 to 4.5 μs after the laser pulse, which will later be shown to be a range of good sensitivity to temperature at engine conditions while staying within the time window between blade passages. Prior to fitting, the DC baseline, obtained from averaging the pre-pulse portion of the data, was subtracted off. This two-parameter curve fit resulted in extracted values of the pre-exponential constant (S_0) and lifetime (τ) for each decay.

Two blades of the high-pressure turbine disk were used for the measurements and each was coated with a 25 μm-thick phosphor layer on top of a 200 μm thick yttria stabilized zirconia TBC. The phosphor layer on one blade was a YAP:Tm coating deposited by electron beam physical vapor deposition (EB-PVD), and on the other blade was a YAG:Dy coating,

Table 1. Fit parameters in equations (5) and (6) for the calibration data of the two phosphor-coated turbine blades.

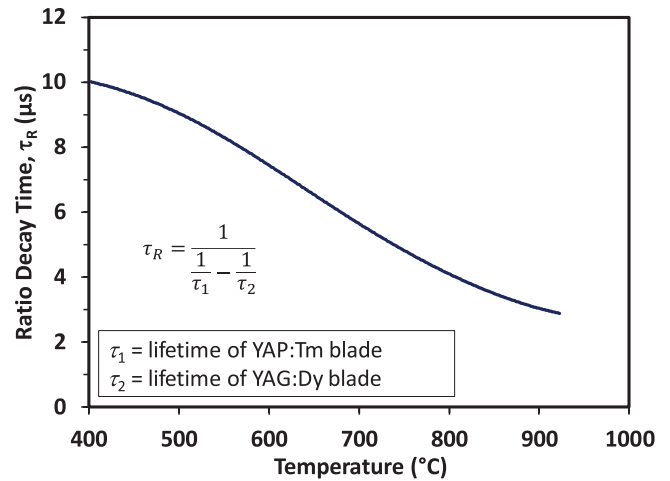| Fit parameter	YAP:Tm	YAG:Dy
τ_{rad}	9.184 μs	72.94 μs
α	545.3	—
α_1	—	742.6
α_2	—	1.303×10^{13}
ΔE	4406 cm^{-1}	—
ΔE_1	—	5046 cm^{-1}
ΔE_2	—	24 740 cm^{-1}

Figure 3. Calibration curve for the ratio decay time, derived from the YAP:Tm/YAG:Dy phosphor pair.

deposited by the solution precursor plasma spray method [21]. Figure 2 shows lifetimes obtained from the two phosphor coated blades, in which the data are shown as black squares and curve fits are shown as white lines. The temperature dependence of the decay from the YAP:Tm-coated blade, $\tau(T)$, could be fit well by a simple thermal activation energy model:

$$\tau = \frac{\tau_{rad}}{1 + \alpha e^{-\Delta E/kT}} \tag{5}$$

where τ_{rad} is the non-temperature-sensitive radiative decay rate, $\alpha = \tau_{rad}/\tau_{nr}$, where τ_{nr} is the temperature-dependent nonradiative decay time, ΔE is the activation energy, and k is the Boltzmann constant. Because the decay from the YAG:Dy-coated blade was more complex, its temperature dependence could not be fit well using a single thermal activation energy, so a dual thermal activation energy model was used to achieve a better fit:

$$\tau = \frac{\tau_{rad}}{1 + \alpha_1 e^{-\Delta E_1/kT} + \alpha_2 e^{-\Delta E_2/kT}} \tag{6}$$

where ΔE_1 and ΔE_2 are the two activation energies, $\alpha_1 = \tau_{rad}/\tau_{nr1}$, $\alpha_2 = \tau_{rad}/\tau_{nr2}$, and τ_{nr1} and τ_{nr2} are the two nonradiative decay times. The resulting fit parameters for each phosphor are given in table 1. It should be stressed that these models are only intended to provide good fits to the data and that the fit parameters may not be physically meaningful. The selected fit range of 1 to 4.5 μs after the laser pulse occurs during the initial, faster portion of the YAG:Dy decay and
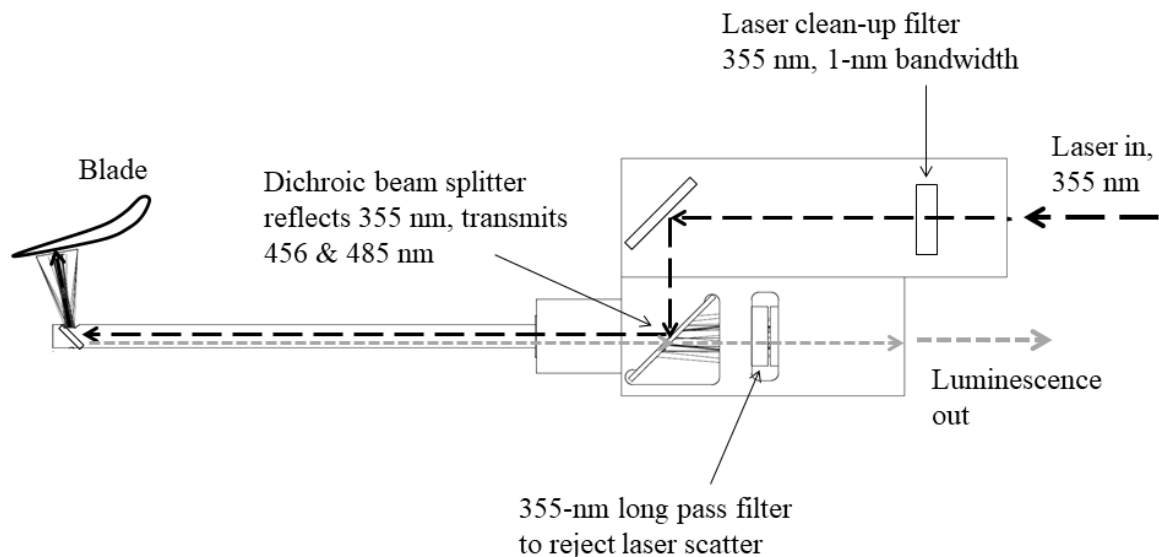
Figure 4. Probe for measuring turbine blade temperature in an engine using thermographic phosphors.

therefore the lifetime values plotted in figure 2 are much shorter than values typically reported in the literature for this phosphor. While the YAG:Dy-coated blade exhibited the desired longer decay compared to the YAP:Tm-coated blade, the YAG:Dy initial decay used here did not show the desired delayed onset of temperature sensitivity to 1100 °C that the longer term YAG:Dy decay is known to exhibit. Still, the decay time characteristics were acceptable.

A calibration curve for the effective decay lifetime of *R* was constructed from the calibration curves of the individual phosphors and is shown in figure 3. This curve was obtained by computing $\tau_R = (1/\tau_1 - 1/\tau_2)$ at each temperature in the range 400 °C to 920 °C. It can be seen that every value of τ_R within this range has a corresponding unique temperature. The effects of the individual decays can be observed in the τ_R temperature dependence as follows. The initial downturn to higher temperature sensitivity at about 500 °C in figure 3 corresponds to the onset of YAP:Tm temperature sensitivity in figure 2, and the upturn to lower temperature sensitivity at about 800 °C in figure 3 corresponds to the onset of steep temperature dependence of YAG:Dy in figure 2. Overall, the ratio decay time, τ_R, can be seen to have a reasonable sensitivity over the range 400 °C to 900 °C.

3. Experiment

The technique was implemented in a turbofan aircraft engine from a business jet with an approximate thrust of 4000 lb$_f$ using a custom probe, which is shown in figure 4. The probe consisted of a beamsplitter housed in a rugged casing attached to an endoscope that relayed the laser beam to the measurement location and transmitted the collected luminescence to a fiber optic bundle attached to the photomultiplier tube mentioned earlier, located outside the engine. Thus, no alignment of beams into the engine was required, and all light passed into and out of the engine via fiber optics. Light from a 355 nm pulsed laser (pulse energy 6 mJ, pulse duration

10 ns, pulse repetition rate 10 Hz) provided the excitation, and a dichroic beamsplitter was used to separate the excitation beam from the collected signal beam. The beam exiting the laser was coupled into a fiber optic that had an efficiency of about 50% and thus delivered about 3 mJ to the measurement spot, which was about 7 mm in diameter. A narrowband laser clean-up filter, centered at 355 nm with a 1 nm bandwidth, was used to remove unwanted Raman scattering, which otherwise resulted from the laser delivery fiber. A prism at the tip of the probe turned the excitation and signal collection beams by 85°, as shown in figure 4, enabling the measurement region to be viewed from this angle. Signals from the photomultiplier tube were digitized at a rate of 100 MSamples s^{-1} by the oscilloscope mentioned earlier and transferred to a computer via GPIB. Various bandpass filters were used at the photomultiplier to select the desired luminescence band depending on the phosphor under interrogation.

The two blades were adjacent to each other with an angular separation of 8°. The probe was inserted radially into the turbine case and protruded a few millimeters into the flow path between the high and low-pressure turbine disks. It viewed the suction side of the high-pressure turbine blades with a standoff distance of about 25 mm.

Synchronization of the laser with the engine was accomplished using a multichannel delay generator (Berkeley Nucleonics BNC-575) that was triggered by a once-per-rev signal from the engine provided by a proximity probe. Pulses were sent from the delay generator to the laser to fire the laser flashlamps and *q*-switch when the desired blade was within the field of view of the probe. In this way, the desired blade could be selected by properly setting the laser timing delay. Data collection occurred while the engine was operating in a steady mode, and consisted of setting the delay to correspond to first the YAP:Tm blade, acquiring a sequence of data, then changing the delay to correspond to the adjacent YAG:Dy blade and acquiring again. The delay time offset between the blades was chosen to exactly correspond to 8° angular rotation
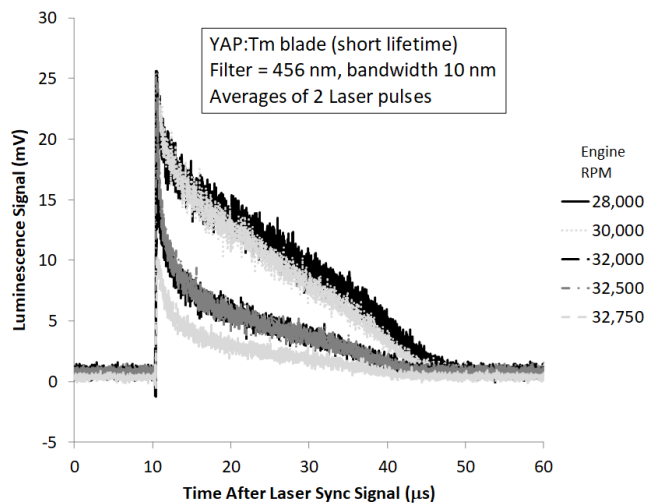
Figure 5. Luminescence from a YAP:Tm-coated turbine blade in an operating engine using a bandpass filter at 456 nm, averages of two laser pulses.

so that data collection for each blade was performed over the same range of motion of the blade passing in front of the probe in order for the effects of motion, $\Omega(t)$, to cancel out of the ratio measurement given by equation (2). The process of acquiring data from both blades took about five minutes.

4. Results and discussion

Figure 5 shows raw data acquired during engine operation from the YAP:Tm-coated blade, which is the fast-decaying phosphor, using a 10 nm bandwidth filter centered at 456 nm on the photomultiplier tube. The vertical axis is the luminescence signal measured by the photomultiplier tube in volts, and the horizontal axis is the time after a sync signal that was generated about 10 μs before the laser pulse. The curves are color coded to indicate engine speed in revolutions per minute, as indicated in the legend. Each curve is a phase average of two laser pulses while the laser was firing at a repetition rate of 10 Hz. Considering the averaging, the effective measurement update rate was 5 Hz, and the signal voltages were digitized and stored on the computer. A load resistance at the oscilloscope of 50 ohms was used, corresponding to an RC time constant of about 60 ns. A small DC offset was intentionally added via the oscilloscope to raise the signal level above zero to avoid losing data when taking the logarithm for later analysis. Similar data (not shown) was obtained from the same blade using a bandpass filter at 365 nm, which had similar decay rates but had signal levels that were weaker by about a factor of five.

Figure 7 shows luminescence signals from the same blade during the engine test averaged over 200 laser pulses. The portion of the data just before the laser pulse was used for determining the DC baseline, which was subtracted off before plotting. Figure 7 reveals that most of the temperature dependence seems to reside within the first 5 μs. This can be observed considering two regions, marked '1' and '2' in figure 7, in which the slopes of the curves in region 1 vary significantly, as
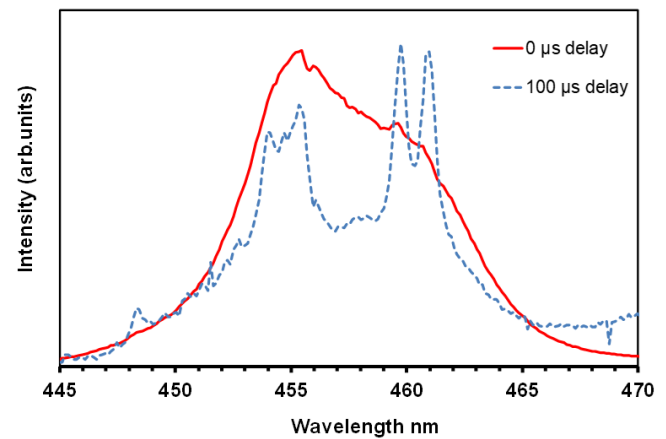

Figure 6. Time-resolved emission spectra from nominal YAP:Tm coated blade obtained 0 μs (2.5 μs duration) and 100 μs (10 μs duration) after 355 nm excitation pulse.

indicated by black lines, presumably due to different temperatures at the different engine settings, but the slopes in region 2 are all quite similar. This behavior suggests that in addition to the temperature dependent decay with timescales on the order of a few microseconds, there was a temperature independent longer-lived component. The source of the longer-lived component was found to be a significant fraction of YAG:Tm (confirmed by x-ray diffraction) present in the nominal YAP:Tm blade coating. Time-resolved emission spectra were obtained, shown in figure 6, which revealed that spectral emission at long decay times was dominated by YAG:Tm.

The presence of both YAP and YAG phases from the Y_2O_3–Al_2O_3 phase system is most likely a consequence of different rates of evaporation among the constituents of the ingot during coating deposition by EB-PVD. Since the phosphor-coated blades were themselves used in both the calibration and engine measurements, any effects from the YAG phase on the decay time would be the same in both cases. Therefore, no errors specifically due to the presence of YAG are expected in the engine measurements. However, the shorter lifetimes of YAP:Tm are more beneficial from a measurement precision standpoint. Therefore, for the determination of temperature, data from this longer-lived YAG:Tm dominated region was discarded and only the shorter lived YAP:Tm-dominated data from region 1 was used.

Figure 8 shows data from the adjacent YAG:Dy blade during the engine tests, which is the more slowly decaying phosphor. Two wavelength bands of the luminescence spectrum were investigated, centered at 456 nm and 485 nm, but only the data taken at 485 nm are shown. The data from 456 nm was similar in shape but had signals that were weaker by about a factor of four. Note that the effect of blade motion is very evident as observed by the initial increase in luminescence intensity as the blade moves towards the detector. Figure 8 is best understood by considering figure 1, which shows the geometry of the light collection system. It shows that the solid angle of collection is not constant but varying in time as the blade moves towards the probe. The increasing collection angle can cause the signal to rise, even though it is experiencing a natural decay after the laser pulse. If the
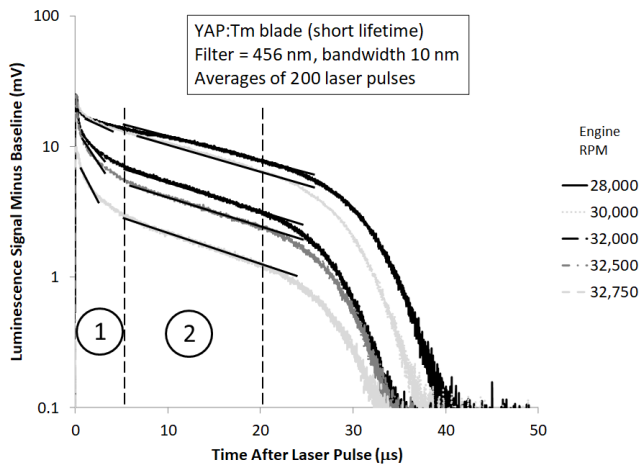
Figure 7. Averaged luminescence from a YAP:Tm-coated turbine blade in an operating engine filtered at 456 nm, averages of 200 laser pulses.
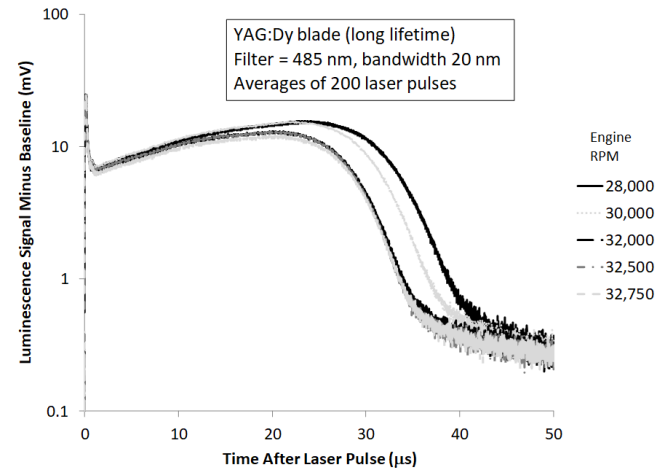

Figure 9. Averaged luminescence from a YAG:Dy-coated turbine blade in an operating engine filtered at 485 nm, averages of 200 laser pulses.
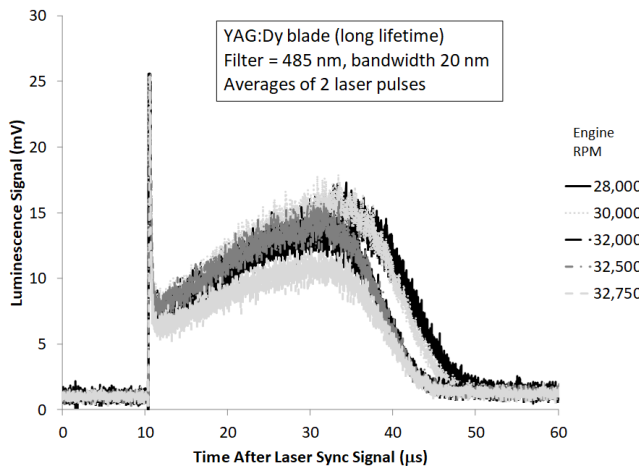

Figure 8. Luminescence from a YAG:Dy-coated turbine blade in an operating engine using a bandpass filter at 485 nm, averages of two laser pulses.

Figure 10. Ratio of luminescence signals from YAP:Tm blade (filtered at 456 nm) to the YAG:Dy blade (filtered at 485 nm).

effect of increasing solid angle is great enough to overcome the decrease due to natural luminescence decay, there will be a rise in signal with time, at least until the blade passes the probe and the signal disappears.

Figure 9 shows luminescence data from the YAG:Dy blade during the engine tests phase averaged over 200 laser pulses. The signal can be seen to increase with time as the blade moves closer to the probe, as described above and shown in figure 1. After the initial spike in the signal, which is due to laser light scattering off the blade, the luminescence signal rises to a maximum of 2.3 times the value at the start, consistent with the geometric analysis described in section 2.1.

At a given engine speed, the data from the two blades were collected about five minutes apart. During this time, the engine was at a stable operating condition, so the temperatures of the blades can be assumed to be the same. Thus, the ratio of luminescence signals from the two blades should be a valid way of determining the temperature in this case, and time decays of this ratio are shown in figure 10 for a range of engine speeds. In each case, the ratio reaches a peak within one microsecond
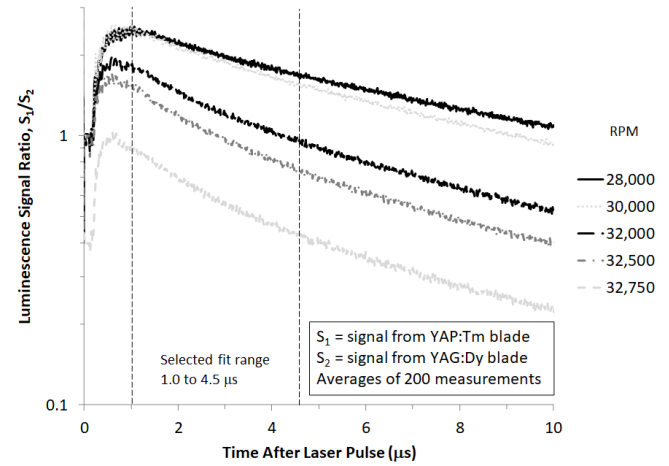
after the laser pulse, and then decays with time. The decay curves were approximated as single-exponential functions of the form given by equation (2), and the corresponding effective lifetimes were obtained from curve fits over the range of 1.0 to 4.5 μs after the laser pulse. This range was selected because it provided good sensitivity to temperature, and should be least affected by the longer-lived YAG:Tm luminescence mentioned above.

Values of τ_R were extracted by fitting the data shown in figure 10 to equation (2), and the calibration curve of figure 3 was used for converting these lifetimes to temperatures. Predicted temperatures were provided by the engine manufacturer, which were derived from a 1D analysis based on the engine thermodynamic cycle model. Figure 11 shows temperatures obtained from the thermographic phosphors (TP), which range from 513 °C to 767 °C, plotted together with the predicted temperatures over a range of engine speeds.

Due to difficulties in predicting the combustion gas temperatures, the values shown as 'predicted' in figure 11 are understood to be approximations. Therefore, the predictions are not exact, and the measured temperatures are considered to be in
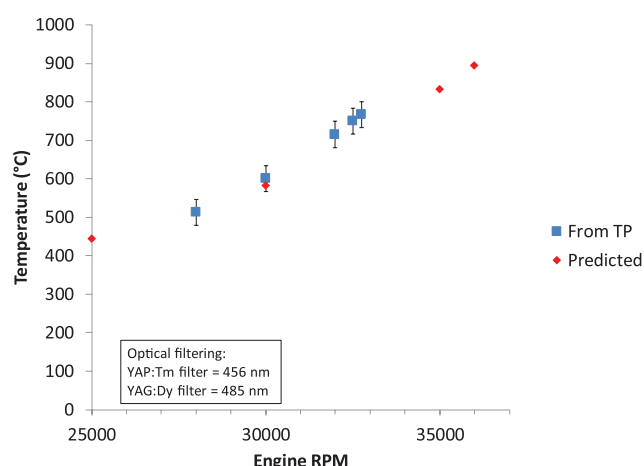
Figure 11. Temperatures measured by thermographic phosphors (TP) and predicted in an aircraft turbofan engine.

good agreement with them. Error bars are shown for the TGP measurements based on the reproducibility of the calibration curves. The TGP data show the same trend as the predictions, but the temperatures are about 25 °C greater, which is within the measurement error. No correction has been made for small differences in decay time that can occur at temperatures above 750 °C for YAG:Dy due to differences in oxygen quenching [6, 22] and may also occur for YAP:Tm. Differences in oxygen content between the calibration furnace and engine environments can lead to small differences in decay time at high temperature, but the difference has been shown to be above a few percent only at the very low oxygen concentrations [22] that might be attained in rich-burn engine environments. Temperature measurements were somewhat limited by the 'contaminating' long-lived YAG:Tm contribution to the decays measured from the nominal YAP:Tm blade coating. Because of the long-lived YAG:Tm decay component, the decay curve fitting window could not be extended beyond 4.5 μs and therefore could not include the later stages of the YAP:Tm decay in the fitting window (figure 10). Single phase YAP:Tm coatings would improve the temperature measurement range and accuracy, and extended temperature range phosphors like Y_2O_3:Er would enable temperature measurements from engine off to maximum engine power [23].

The effective measurement time is limited by the fact that the data from each blade were acquired in sequence, with a delay between measurements on different blades on the order of a few minutes in this demonstration. A possible method for enabling shorter measurement times may be to create a phosphor coating containing both short and long lifetime components in a single coating, the luminescence from which can be separated out spectrally at the detector. This suggestion could enable single-shot measurements of temperature that may be useful for measuring transient events.

5. Conclusions

A method of phosphor thermometry was introduced in which the effects of motion on the time-dependent signals was compensated for by utilizing the ratio of the response of a temperature-sensitive short-lifetime phosphor to that of a less sensitive long-lifetime phosphor. Temperature measurements on moving turbine blades during engine operation were demonstrated and found to be within 25 °C of those estimated by the engine manufacturer over a range of engine operating conditions, which is within the measurement error. The method requires two phosphor-coated blades to be at the same temperature during the measurement, requiring steady engine conditions during data collection. Future variations may be developed for mixtures of phosphors to enable simultaneous long and short lifetime measurements from the same blade, which should enable simpler and faster measurements.

ORCID iDs

Thomas P Jenkins ⬦ https://orcid.org/0000-0001-8045-8780
Stephen W Allison ⬦ https://orcid.org/0000-0002-5887-5403
Jeffrey I Eldridge ⬦ https://orcid.org/0000-0002-7928-4530

References

[1] Koff B L 2004 Gas turbine technology evolution: a designer's perspective *J. Propul. Power* **20** 577
[2] Kerr C and Ivey P 2002 An overview of the measurement errors associated with gas turbine aeroengine pyrometer systems *Meas. Sci. Technol.* **13** 873
[3] Feist J P, Heyes A L and Nicholls J R 2001 Phosphor thermometry in an electron beam physical vapour deposition produced thermal barrier coating doped with dysprosium *Proc. Inst. Mech. Eng.* G **215** 333
[4] Eldridge J I, Bencic T J, Allison S W and Beshears D L 2004 Depth-penetrating temperature measurements of thermal barrier coatings incorporating thermographic phosphors *J. Therm. Spray Technol.* **13** 44
[5] Gentleman M M, Eldridge J I, Zhu D M, Murphy K S and Clarke D R 2006 Non-contact sensing of TBC/BC interface temperature in a thermal gradient *Surf. Coat. Technol.* **201** 3937
[6] Brübach J, Pflitsch C, Dreizler A and Atakan B 2013 On surface temperature measurements with thermographic phosphors: a review *Prog. Energy Combust. Sci.* **39** 37
[7] Eldridge J I 2018 Single fiber temperature probe configuration using anti-Stokes luminescence from Cr:GdAlO3 *Meas. Sci. Technol.* **29** 065206

[8] Allison S W, Goedeke S M, Cates M R, Bonsett T C, Smith D E, Brewington A and Bencic T J 2005 Phosphor thermometry in an operating turbine engine *41st AIAA/ ASME/SAE/ASEE Joint Propulsion Conf. & Exhibit* 2005–4374

[9] Peng D, Yang L, Cai T, Liu Y and Zhao X 2016 Phosphor-doped thermal barrier coatings deposited by air plasma spray for in-depth temperature sensing *Sensors* **16** 1490

[10] Yang L, Peng D, Zhao C, Xing C, Guo F, Yao Z, Liu Y, Zhao X and Xiao P 2017 Evaluation of the in-depth temperature sensing performance of Eu- and Dy-doped YSZ in air plasma sprayed thermal barrier coatings *Surf. Coat. Technol.* **25** 210

[11] Noel B W, Turley W D and Allison S W 1994 Turbine-engine applications of thermographic-phosphor temperature measurements *Conf.: Remote Temperature Sensing Workshop*

[12] Heyes A L, Feist J P, Chen X, Mutasim Z and Nicholls J R 2008 Optical nondestructive condition monitoring of thermal barrier coatings *J. Eng. Gas Turbines Power* **130** 061301

[13] Abou Nada F, Lantz A, Larfeldt J, Markocsan N, Aldén M and Richter M 2016 Remote temperature sensing on and beneath atmospheric plasma sprayed thermal barrier coatings using thermographic phosphors *Surf. Coat. Technol.* **302** 359

[14] Jenkins T P, Allison S W and Eldridge J I 2013 Measuring gas turbine engine component temperatures using thermographic phosphors *SPIE Newsroom* (https://doi.org/10.1117/2.1201303.004769)

[15] Eldridge J I, Jenkins T P, Allison S W, Cruzen G S, Condevaux J J, Senk J R and Paul A D 2011 Real-time thermographic–phosphor-based temperature measurements of thermal barrier coating surfaces subjected to a high-velocity combustor burner environment *57th Int. Instrum. Symp.* (New York: Curran) pp 208–28

[16] Jenkins T P, Eldridge J I, Allison S W, Howard R P, Jordan E H and Wolfe D E 2013 An experimental investigation of luminescence lifetime thermometry for high temperature engine components using coatings of YAG:Dy and YAG:Tm *Joint Conf. 67th Mach. Fail. Prevent. Technol. MFPT 2013 and 59th Int. Instrumentation Symp. ISA* (Cleveland, OH)

[17] Eldridge J I, Allison S W, Jenkins T P, Gollub S L, Hall C A and Walker D G 2016 Surface temperature measurements from a stator vane doublet in a turbine afterburner flame using a YAG:Tm thermographic phosphor *Meas. Sci. Technol.* **27** 125205

[18] Cash C A, Allison S, Hayes B and Niska H 2013 Versatile affordable advanced turbine engine (VAATE), phase I and II, delivery Order 0002: gas turbine engine sensor and instrumentation development *Final Report* AFRL-RQ-WP-TR-2013-0275 (Global Security, Alexandria, VA)

[19] Feist J P, Sollazzo P Y, Berthier S, Charnley B and Wells J 2012 Application of an industrial sensor coating system on a Rolls-Royce jet engine for temperature detection *J. Eng. Gas Turbines Power* **135** 012101

[20] Amiel S, Copin E, Sentenac T, Lours P and Le Maoult Y 2018 On the thermal sensitivity and resolution of a $YSZ:Er^{3+}/YSZ:Eu^{3+}$ fluorescent thermal history sensor *Sensors Actuators* A **272** 42

[21] Chen D, Jordan E H, Renfro M W and Gell M 2000 Dy:YAG phosphor coating using the solution precursor plasma spray process *J. Am. Ceram. Soc.* **92** 268

[22] Ishiwada N, Tsuchiya K and Yokomori T 2019 Applicability of Dy-doped yttrium aluminum garnet (YAG:Dy) in phosphor thermometry at different oxygen concentrations *J. Lumin.* **208** 82

[23] Eldridge J I 2019 Luminescence decay-based Y_2O_3:Er phosphor thermometry: Temperature sensitivity governed by multiphonon emission with an effective phonon energy transition *J. Lumin.* **214** 116535